The modelling of splitting destruction of barriers from anisotropic materials in 3D

M.N. Krivosheina[1,a], M.A. Kozlova[1,b], H.V. Tuch[1,c], S.V. Kobenko[2,d],

[1]Institute of Strength Physics and Materials Science SB RAS, 2/4, pr. Akademicheskii, Tomsk, 634021, Russia

[2]Nizhnevartovsk State University of Humanities, Nizhnevartovsk, 56, Lenin St., 628605, Russia

[a] marina_nkr@mail.ru, [b] kozlova_ma@mail.ru, [c] elenatuch@yandex.ru, [d] sergeyvk@inbox.ru

Keywords Computer simulation, impact loading, anisotropy, spallation fracture

Abstract

Depending on kinematic or geometric parameters of the stressing of barriers, their deterioration may happen as a result of cratering, fuse blowing, formation of a spalling plate, etc. For the purposes of modelling simulation of various types of deterioration, it is important to use different criteria of deterioration. This work offers an approach to the modelling of slabbing deterioration of barriers allowing for the anisotropy of elastic and plastic properties of barrier materials.

The equations of continuum mechanics are means of modelling the kinetics of formation, development, and fusion of micropores in waves of tension. The presented computation model of the deterioration of anisotropic materials in waves of tension consists of two parts, which are 1) equations describing the law of development of discontinuity flaws (pores of spherical shape) and 2) equations defining the behaviour of the elastoplastic material, taking into account changes in mechanical properties (elastic and plastic ones) due to the formation and development of a great number of pores right up to the deterioration of the material.

Introduction

Even normal impact loading causes three-dimensional stress state in the obstruction. Spallation fracture in engineering materials with zonal, structural and crystallographic heterogeneity depends on the quality of the material. Spallation fracture velocity depends on applied stress and is proportional to concentration of fracture nuclei and their average growth rate. Zonal heterogeneity is determined by ingot technology and pressure shaping. Ingot manufacturing is accompanied by heterogeneous distribution of alloying agents and inevitable impurities in cast zones (surface, central, upper and bottom) and inside crystallites. An additional problem is original porosity and contraction cavities which make several percents in casting blocks. When these materials are rolled, some pores are sealed, while the rest of them are transformed into the system of flat cracks along rolling direction and vertical to estimated loading. Thus it leads to significant anisotropy in mechanical properties in the plane and through the thickness of the cast. Spallation strength evaluation makes it possible to determine the performance level of the structure made of such materials. But all experimental techniques used to research spallation fracture phenomena provide only indirect information about fractures process and stresses.

Computer simulation of dynamic deformation and spallation fracture of engineering elastoplastic materials makes it possible to get the spallation fracture model independent from material deformation model. The research uses spallation fracture criterion modified by critical level of deformation by Johnson G.N. [1] Heterogeneous porous anisotropic medium is viewed as a two-component material, consisting of the matrix and inclusions, i.e. pores. Forgetting surface energy of pores and gas pressure in them, we see that porous material pressure is

determined though matrix pressure and porosity. The equation to describe porosity variance in the material is obtained from the solution of a single pore deformation under hydrostatic tension in dynamic approximation [2]. It is supposed that departures from spherical shapes of pores in an anisotropic material can be ignored. This sets certain limits for model validity: the model is can be applied to calculate fracture of porous materials with low anisotropy of plastic properties, such as that of metals and alloys.

The continual-kinetic approach is used to simulate fracture as a continuous process of damage accumulation by means of aggregate parameters. Material fracture under tension is the process of formation, merging and growth of micropores. The net effect of micropores on stress state of the medium consists in lower values of mechanical properties due to smaller effective cross-section plane in the porous material though which the loading is transmitted. The peculiarity of plastic deformation of porous solids is that it is accompanied by irreverible change in volume, besides, plastic deformation depends on hydrosatic stress component, i.e. even hydrostatic stress component can cause plasticity. In case of high concentration of micorpores in the cell the distance between neighboring mocroppores becomes proportionate to their size. Besides, due to the chaotic distribution of micropores it is possible for the neigboring micorpores to be closer to each other. It leads to assumption of micropores interaction when they reach critical concentration followed by their merge and, in the long run, by aperture of continuity between pores in the cell. The cell gets a fracture with the size equal to characteristic cell size.

In the statement of the problem simulation of deformation and fracture in isotropic and anisptropic materials differs only in connection between stresses and deformation. Mathematic simulation is performed within continuum mechanics. The set of equations to describe the motion of compressible medium includes the following equations: continuity equation, motion equation and energy equation [3].

The model is used based on one of the first porous medium models. From Carroll-Hault model we use the equation of state for porous materials taken as

$$P = \frac{f(V/\alpha, E)}{\alpha}, \tag{1}$$

which makes it possible to take into account smaller effective cross-section area through which the load in a porous material is transmitted [4]. Here P is hydrostatic pressure, V is volume, α is porosity, E - specific internal energy.

The damage is measured by means of porosity factor originally proposed by Herrman [5]. This is the relation of specific volume of porous medium $(V = V_m + V_p)$ to the specific volume of the solid material matrix (basic material):

$$\alpha = V \diagup V_m . \tag{2}$$

In the assumption that changes in porosity depend on plastic properties of the material and do not depend on viscosity, we have the equation of pressure increment obtained with the help of equation-of-state for matrix material and due to spherical pore growth [2]:

$$P \pm \frac{\alpha_s}{\alpha} ln \frac{\alpha}{\alpha - 1} = 0. \tag{3}$$

The symbol "–" is to be placed for stretched porous material, the symbol "+" – for compressed porous material. The calculation of porosity factor is followed by that of density

$$\rho = \frac{\rho_m}{\alpha} \tag{4}$$

and pressure

$$P = \frac{P_m(\alpha\rho,\varepsilon)}{\alpha} \quad (5)$$

In the porous material, where ε - specific internal energy, ρ_m .and P_m - density and pressure of the matrix material.

The total volume of porous anisotropic medium changes under applied stress as the pore and matrix volumes change. We assume that for complex stress in material with low anisotropy of plastic properties the uniform straining of material corresponds to homogenous stress. This means conformance of ball components of stress tensors with straining. The pore volume changes under the impact of hydrostatic stress. Departures from spherical shape of micropores can be ignored. That is why composite stress tensor can be split into ball and deviatoric components:

$$\sigma^{ki} = -P\delta_{ki} + S^{ki} \quad (6)$$

The ball component of the stress tensor is determined from the equation-of-state, the same as for isotropic material. The deviatoric component of the stress tensor in plastic deformation area is determined on the basis of associated flow rule as:

$$\varepsilon_{ij}^{p} = d\lambda \frac{\partial F}{\partial \sigma_{ij}} \quad (7)$$

where $d\lambda = 0$ at elastic strain, always positive in case of plastic deformation, determined by means of plasticity condition, ε_{ij}^{p} – plastic deformation velocity components, F – plasticity as the plasticity condition we take Mises-Hill criterion for anisotropic materials.

The values of components in the matrix of elastic constants (D_{0ij}) and plastic properties (σ_{0ij}) in porous anisotropic material due to microstructural changes in the material change in conformity with changes in porous medium:

$$D_{ij} = D_{0ij}\left(1 - \frac{\alpha-\alpha_{00}}{\alpha_k-\alpha_{00}}\right) \quad (8)$$

$$\sigma_{ij} = \sigma_{0ij}/\alpha \quad (9)$$

where α_{00} – original porosity of material, which remains after compressing strain applied, $\alpha_к$ – threshold porosity followed by fracture, α_s - yield point of the material equal to 2/3 of the material stretching strain. It can vary on the basis of experimental data for calculation purposes.

Statement of problem

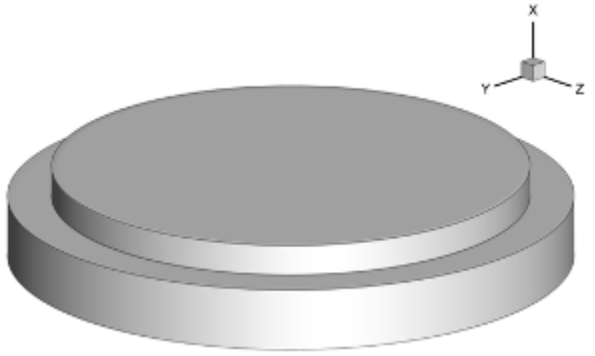

Fig. 1. Volumetric initial configuration of the striker and barrier

The initial conditions ($t = 0$) are:

$\sigma^{ij}=P=E=0$ for $(x,y,z)\in D_1\cup D_2$, $i, j = x, y, z$

$u=\upsilon_0 l_\upsilon$, $v=\upsilon_0 m_\upsilon$, $w=\upsilon_0 n_\upsilon$, for $(x,y,z)\in D_1$

$u=v=w=0$ for $(x,y,z)\in D_2$

$\rho=\rho_i$ for $(x,y,z)\in D_i$, $i=1,2$.

here u, v, w are the components of the velocity vector over the axes X, Y, Z - respectively.

Boundary conditions are: on the free surfaces Σ_1, Σ_2 the conditions of a free boundary are realized: $T_{nn} = T_{ns} = T_{n\tau} = 0$ for $(x,y,z)\in\Sigma_1\cup\Sigma_2$

on the contact surface between the striker and barrier the slip condition without friction is realized: $T_{nn}^{+} = T_{nn}^{-}, T_{n\tau}^{+} = T_{n\tau}^{-} = T_{ns}^{+} = T_{ns}^{-} = 0, v_n^{+} = v_n^{-}$ for $(x,y,z)\in\Sigma_3$.

Here n- is the unit vector of the normal to the surface at the point considered; τ1 and τ2 are the mutually perpendicular unit vectors in the plane tangent to the surface at this point; T_n is the vector of the force on the elemental area with the normal n, and υ is the velocity vector. The subscripts of the vectors T_n and υ mean the projections to the corresponding vectors of the basis; the sign "+" characterizes the value of the parameters in the striker, the sign "–" — in the barrier.

Spall fracture of transtropic barrier materials in the plane of isotropy

Spall fracture transtropic barriers considered by the example of aluminum alloy 2024. Characteristics of target material of aluminum alloy 2024 following: the characteristics of elasticity in the direction of the axes OX, OY и OZ: $E_x = 86700MPa$; $E_y = 92100MPa$; $E_z = 92100MPa$; $G_{xy} = 33000MPa$; $G_{zx} = 33000MPa$; $G_{yz} = 31000MPa$, $\nu_{xy} = 0.32$, $\nu_{zx} = 0.34$, $\nu_{yx} = 0.33$

characteristics of plasticity

$\sigma_{sx} = 290MPa$, $\sigma_{sy} = 350MPa$, $\sigma_{sz} = 350MPa$, $\tau_{sxy} = 150MPa$, $\tau_{szx} = 150MPa$, $\tau_{syz} = 180MPa$

constant of the isotropic hardening ξ =5.5.

We used the following constants of the equation of state in the form of Mie-Grüneisen

$$P = \sum_{n=1}^{3}\left(\frac{V}{V_0}-1\right)^n\left[1-K_0\left(\frac{V}{V_0}-1\right)/2\right]+K_0\rho E,$$

$\gamma_0 = 2.13$, $K_1 = 74400$, $K_2 = 53200$, $K_3 = 30500$

Here E_i – Young's modulus, G_{ij} – shear modules, ν_{ij} – Poisson's ratios. That is along the axis OX material is reduced with respect to the mechanical properties of the material properties in the direction of axes *OY* and *OZ*. Impact loading of plates transtropic alloy is produced in the direction of the *OX* at the same projectile material - an isotropic aluminum alloy with the following characteristics:

$E_x = 86700MPa, G_{xy} = 33000MPa, \sigma_{sx} = 290MPa, \xi$ =5.5;

We simulate impact loading of the obstruction 10 mm thick, 90 mm in diameter using a disk 5 mm thick, 76 mm in diameter. The initial velocity of the ram tester is 500 m/s. In case of impact loading of the obstruction made of transtropic materials, obstruction fracture process is close to axisymmetric, if the direction of impact loading coincides with the singular axis of the obstruction material. Fig. 2 shows velocity component distribution on the back surface of the obstruction along the impact direction at 6 mcs of the process. At this moment of time the central section of the obstruction back surface shows velocity higher than 450 m/s.

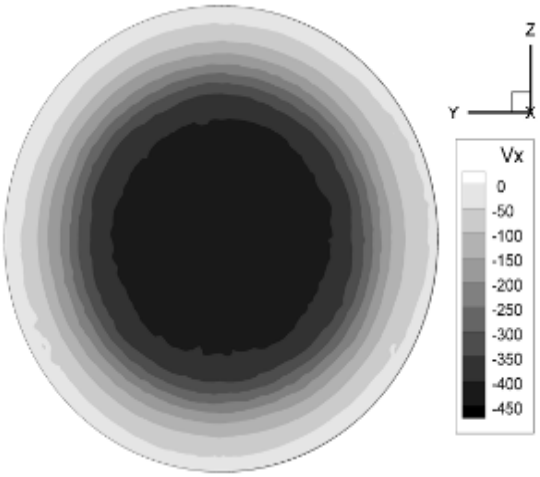

Fig. 2. Velocity component distribution along impact direction V_x on the obstruction back surface on 6 mcs of the process; υ_0=500m/s, ultimate porosity α_* =1.43

Distribution velocity component along the impact direction in the spallation plane of the obstruction is given in Fig. 3. The cross-section is shown as a plane and a spallation fracture is in the form of a saucer. That is why in Fig. 3 we can see an annular zone with velocity lower than 50 m/s, as outside the spallation fracture. Figure 3 looks like that due to spallation plane distortion in the course of fracturing as well as complex character of the cross-section in the obstruction, which imitates the shape of spallation fracture zone (Fig.5). Fig. 2 shows that velocity over 400 m/s emerges inside spallation fraction radius. We observe minor velocity fluctuations within 50 m/s in fragments of the fractured material and above the boundaries of the spallation fracture (Fig. 3).

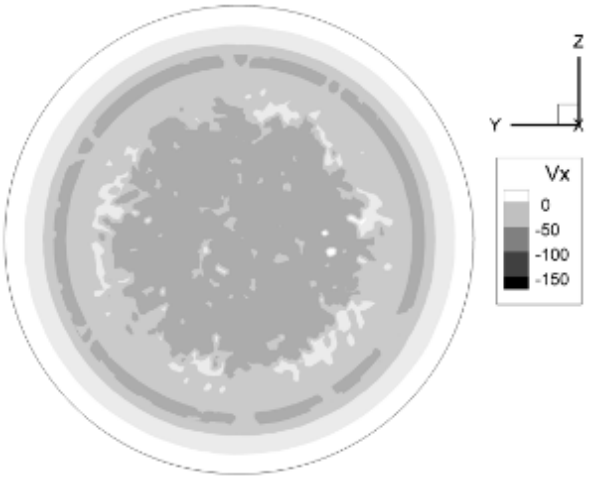

Fig. 3. Velocity component distribution along impact direction V_x on the obstruction spallation plane at 6 mcs of the process; υ_0=500m/s, ultimate porosity $\alpha_* = 1.43$

Fig. 4a shows velocity component distribution along the impact direction in the cross-section of the ram tester and the obstruction at this moment of time. Velocity distribution is axisymmetric with the maximum velocity concentrated in the spallation fracture zone of the obstruction. Fig. 4b shows the shape of the spallation fracture with mass fraction distribution at this moment of time. It is so axisymmetric as in case when isotropic materials are used to simulate obstruction spallation fracture. The central sections of the ram tester and obstruction have bends in opposite directions (Fig. 4a).

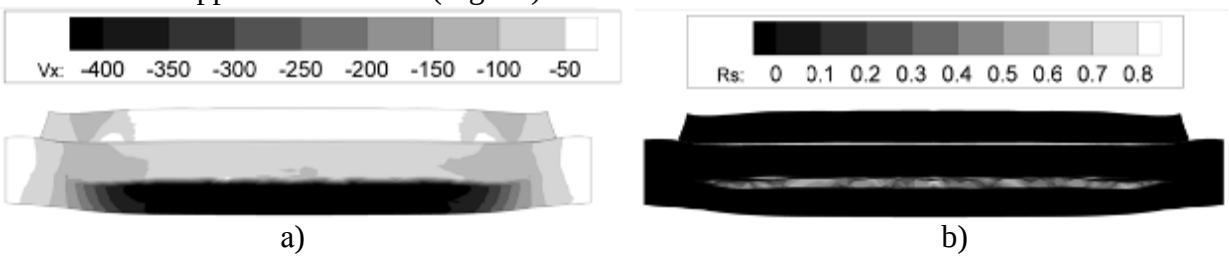

a) b)

Fig. 4. Distribution in the cross-section of the ram-tester and obstruction at 6 mcs of the process: a – velocity components along impact direction, b – mass fractions of the fractures material in spallation plane of the obstruction; υ_0=500m/s, ultimate porosity $\alpha_* = 1.43$

Spallation fracture of the transtropic obstruction in anisotropic plane

This part of the paper deals with spallation fracture in transtropic obstructions made of aluminum alloy 2024 the properties of which completely coincide with those of the aluminum alloy in Fig.2. The material specifications are also oriented to the designed coordinate system as in the statement of the problem (Fig.1). The ram tester initial velocity – 500m/s. The main difference from the problem set in Fig.1 is that now both the front and back surfaces of the obstruction lie in *XOZ* plane and the impact loading of the obstruction is *OY*-directed. Thus, the spallation plane is located in *XOZ* plane, with elastic and plastic properties of the obstruction material in *OX* and *OZ* directions being different. The spallation fracture zone of the material has 3D (nonaxisymmetric) contours.

Nonaxisymmetric porosity distribution in the obstruction material affects stress-strain distribution on the back surface of the obstruction. Stress-stain distribution is most clearly observed in distribution of V_y velocity components along the impact loading direction. As is shown in Fig. 5, the symmetry observed does not coincide with the computational grid symmetry (originally for the construction of the computational grid the back surface of the obstruction was

divided into 6 equal parts). This symmetry is determined by lack of isotropy of mechanical properties of the obstruction material in the spallation fracture plane. In all calculations this symmetry divides the spallation fracture plane into 4 essentially equal parts. Lack of accurate symmetry in velocity component distribution along the impact loading direction is determined by 3D simulation of material fracture.

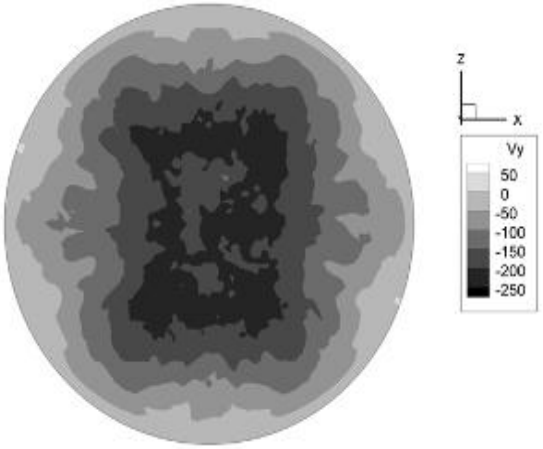

Fig. 5. Velocity component distribution along the impact loading direction on the back surface of the obstruction V_y at 6mcs of the process, υ_0=500m/s, ultimate porosity $\alpha_* = 1.4$

Fracture zone distribution in spallation plane *XOZ* can be observed in the course of cross-section construction in the spallation plane. As the obstruction itself has nonaxisymmetric bend, the thickness of the central section of the spallation in the obstruction makes 2 mm (including the bend) (Fig.4b). The distribution of spallation fracture zones has quadrilateral symmetry in all plane sections within spallation fracture thickness of the obstruction (Fig.6a). Velocity component distribution along the impact loading direction inside the spallation fracture also has quadrilateral symmetry. The fracture zone in the central part of the obstruction has the form close to tetragonal.

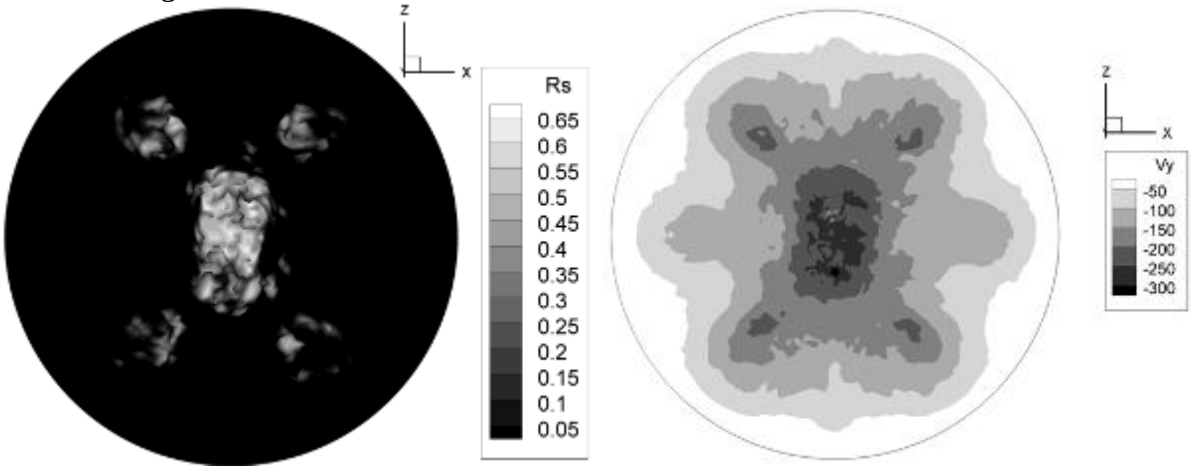

a) b)

Fig. 6 Distribution in the spallation fracture plane at 6mcs of the process: a – spallation fracture zones, b – velocity component V_y ; υ_0=500m/s, ultimate porosity $\alpha_* = 1.25$

Summary

If the material in the spallation fracture plane shows anisotropic mechanical properties, the spallation fracture zone has 3D configuration.

References

[1] Johnson J.N. Dynamic fracture and spallation in ductile solids//J. Appl. Phys. 1981. V. 52. № 4. P. 2812-2825

[2] Belov N.N., Korneev N.N., Nikolaev A. P. Numerical analysis of fracture in plates under the action of pulsed loads // AMTP.– 1985.–№3.– 132–136p.

[3] Sedov L.I. Mechanics of continua. – M.: Nauka, 1976. Vol. 2. – 574p.

[4] Carroll M.M., Holt A.C. //J. Appl. Phys. 1972. V.43 №2 P.1626

[5] Herman B. Constitutive equations for dynamic compression of porous materials\\Mechanics, 1970, № 5, p.96-113